

Performance of an Impulse Radio Communication System in the Presence of Gaussian Jitter

Roman Merz, Cyril Botteron, and Pierre-André Farine
Institute of Microtechnology
University of Neuchâtel, 2000 Neuchâtel
Email: roman.merz@unine.ch

Abstract—In this paper, the bit error rate (BER) performance for an ultra-wide bandwidth (UWB) impulse radio in an additive white Gaussian noise (AWGN) transmission channel and with Gaussian jitter is estimated. The assumed receiver combines the received pulses to increase the signal to noise ratio (SNR) and correlates the received signal with a locally generated template. The resulting performances are discussed separately for a large number and a small number of combined pulses. In the former case, the BER is derived analytically and verified using numerical simulations, and in the latter case, lower bounds for the BER are provided for low and large SNRs. Simulation results are shown to approach asymptotically the provided bounds.

I. INTRODUCTION

UWB impulse radio spreads the energy of the radio signal over a wide bandwidth by transmitting a sequence of pulses with very short duration [1]. Due to the short duration of the pulses (sub-nanoseconds), an accurate time domain analysis is mandatory.

In previous work, the effect of timing jitter on the spectral density has been studied in [2] and [3]. A comparison between the BER of different UWB modulation schemes has been performed in the presence of a uniform timing jitter in static and Rayleigh fading channels in [4]. The BER performance has been studied in correlated random timing jitter in [5]. Jitter models in delay locked loop (DLL) and phase locked loop (PLL) have been used to evaluate the sensitivity of sampling and correlation in a UWB digital receiver in [6]. The BERs for several modulation schemes and various conditions (multipath, multiple-access interference, narrowband interference, and timing jitter) have been evaluated in [7]. The influence of timing jitter on BER in the case of orthogonal Hermite pulse shapes has been studied in [8] and [9]. Finally, using computer simulations, the performance of UWB impulse radio in terms of throughput has been shown sensitive to timing jitter and tracking in [10].

In contrast to the above literature, we investigate in this paper the influence of the jitter on the received signal by assuming that the received pulses are combined to increase the SNR. With this approach, we can thus take into account the effect of the jitter on the coherent combining of the pulses. Based on this time domain analysis, the BER performance is deduced in a second step. This alternative approach complements the existing performance evaluations in the current literature. In addition, lower bounds for the BER for a finite number of combined pulses are derived.

This paper is organized as follows. Section II contains a description of the assumed receiver architecture and provides an integral equation for the BER in the presence of jitter. This equation is solved for special cases in section III. In section III-A, a closed form solution is provided for a large number of combined pulses and in section III-B, two lower bounds are provided for a low number of combined pulses. Both, the closed form solution and the bounds are compared to the outcomes of numerical simulations that are obtained by a Matlab model of the pulse generator, the AWGN transmission channel and a model of the assumed receiver architecture. Finally, the most important results are resumed in section IV.

II. SYSTEM MODEL

We assume an impulse radio UWB communication system using a pulse position data modulation (PPM) and time hopping (TH) code modulation or spreading. However, it is noted that the theory developed in this paper is not restricted to TH, but can also be applied to any other kind of code modulation, as long as the receiver uses the correct code sequence for the code demodulation. The transmitter generates a sequence composed of N_f pulses to transmit the data symbol d_k . In a PPM, the N_f pulses are delayed with respect to the data symbol d_k . Recombining the N_f pulses coherently at the receiver results in a processing gain—denoted as pulse combining gain—and therefore an increase of the SNR at the detector. For the TH, each one of the N_f pulses is delayed with respect to the average pulse repetition interval by $c_j T_c$, where T_c is the chip duration and $\{c_j\}$ for $0 \leq j \leq N_f$ is the spreading sequence characterizing the transmitter of interest. Assuming a pulse shape $p(t)$, the generated signal is written as

$$s(t) = \sum_{k=-\infty}^{\infty} \sum_{j=1}^{N_f} p(t - kN_f T_f - \tau_j - d_k \delta) \quad (1)$$

where the delay due to the TH is $\tau_j = (j-1)T_f - c_j T_c$ and δ is the modulation index. For an AWGN transmission channel, the received signal is

$$r(t) = s(t) + n(t) \quad (2)$$

where $n(t)$ is Gaussian distributed with two-sided noise spectral density $N_0/2$ and mean value 0.

For the performance analysis, we assume a correlation receiver that furthermore coherently combines the N_f pulses. It is

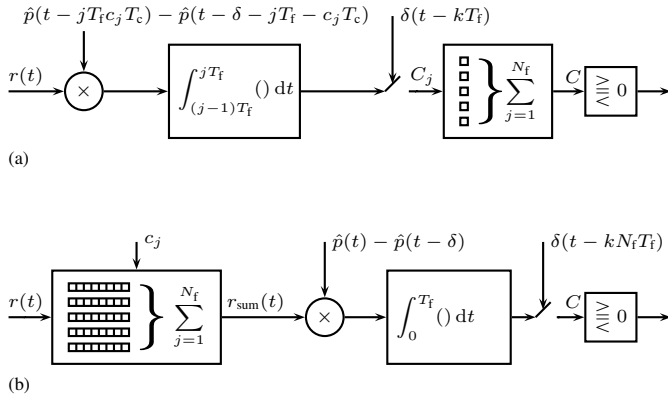


Fig. 1. Architectures for a correlation receiver with pulse combining for equiprobable binary data symbols.

well known that a correlation receiver with a locally generated template matched to the received noiseless signal is optimum in an AWGN transmission channel [11]. Two potential receiver architectures are presented in figure 1. The receiver architecture (a) calculates the j th correlation value C_j between the j th received pulse and the locally generated template and sums the correlation values to obtain the correlation value $C = \sum_j C_j$. Finally, the detector maps the sign of the correlation value to estimate the data symbol d_k . In the architecture (b), the received pulses are shifted accordingly to the spreading sequence $\{c_j\}$ and coherently combined. The resulting signal $r_{\text{sum}}(t)$ is then correlated with the locally generated template. Both receiver architectures have optimum performance for an AWGN transmission channel if the binary data symbols are equiprobable. It is noted, that the implementation complexity of the two architectures may largely differ. As the receiver architectures are mathematically equivalent, the performance analysis for the SNR and the BER can be based upon either of the architectures.

Without loss of generality, the performance estimation is performed for the 0th data symbol ($k = 0$) to simplify the equations. In the presence of a timing error ε_j for the acquisition of the j th pulse, the correlation value C prior to the detector becomes a function of the timing errors ε_j . The evaluation of the correlation value depends on the receiver architecture. For the architecture (a), it is given by

$$C(\varepsilon_1, \dots, \varepsilon_{N_f}) = \sum_{j=1}^{N_f} C_j(\varepsilon_j) \quad (3)$$

where $C_j(\varepsilon)$ results of the correlation between the received signal $r(t)$ during the time interval $(j-1)T_f \leq t \leq jT_f$ and the locally generated template $h_a(t) = \hat{p}(t - jT_f c_j T_c) - \hat{p}(t - \delta - jT_f - c_j T_c)$. For the receiver architecture (b), the correlation value is

$$C(\varepsilon_1, \dots, \varepsilon_{N_f}) = r_{\text{sum}}(t) \circ h_b(t) \quad (4)$$

where the summed signal is

$$r_{\text{sum}}(t) = \underbrace{\sum_{j=1}^{N_f} p(t + \varepsilon_j)}_{s_{\text{sum}}(t)} + \underbrace{\sum_{j=1}^{N_f} n(t + \varepsilon_j)}_{n_{\text{sum}}(t)} \quad (5)$$

for $0 \leq t \leq T_f$, \circ denotes the correlation operator, and the locally generated template is $h_b = \hat{p}(t) - \hat{p}(t - \delta)$. The timing errors ε_j can be due to a jitter in the emitter's or receiver's clock, a mismatch between the two clock frequencies, or a mismatch between the chip duration used in the transmitter and the receiver. As the noise is incoherently summed, the variance of $n_{\text{sum}}(t)$ is N_f times larger than the variance of $n(t)$. In the absence of timing errors, the pulses are coherently combined, such that the pulse amplitude increases with N_f and the received energy per bit with N_f^2 . Hence, the pulse combining results in a gain of the SNR of N_f . In the presence of timing jitter, the pulse combining becomes partially coherent and the resulting pulse combining gain is expected to be inferior to N_f . The probability of an error during the binary data transmission in a communication system using orthogonal modulation in an AWGN transmission channel is given by the Marcum Q function

$$P(C(\varepsilon_1, \dots, \varepsilon_{N_f}), \mathcal{N}_0) = Q\left(\sqrt{\frac{C(\varepsilon_1, \dots, \varepsilon_{N_f})}{\mathcal{N}_0}}\right). \quad (6)$$

The BER of the data transmission with timing error is therefore given by

$$\text{BER} = \int \dots \int_{-\infty}^{\infty} P(C(\varepsilon_1, \dots, \varepsilon_{N_f}), \mathcal{N}_0) \prod_{j=1}^{N_f} f(\varepsilon_j) d\varepsilon_j \quad (7)$$

where $f(\varepsilon_j)$ is the distribution of the random variable ε_j . In the following, (7) will be solved for specific scenarios.

III. PERFORMANCE ESTIMATION

In section III-A, (7) is solved algebraically for large values of N_f . In section III-B, the BER as denoted in (7) is solved with an algebraic approach and by numerical integration for small values of N_f . All the results are compared to the outcomes of a numerical simulation of the impulse radio communication system (see (2)). For all the approaches, we assume a Gaussian distributed period jitter with variance σ^2

$$\varepsilon_j \sim f(\varepsilon_j) = \frac{1}{\sigma\sqrt{2\pi}} \exp\left(-\frac{\varepsilon_j^2}{2\sigma^2}\right). \quad (8)$$

The received pulse is modeled as the 2nd derivative of a Gaussian pulse shape [1], i.e.,

$$p(t) = \sqrt{\frac{4\zeta R \mathcal{E}_b}{3t_n N_f}} \left(\frac{t^2}{t_n^2} - 1\right) \exp\left(-\frac{t^2}{2t_n^2}\right) \quad (9)$$

where $\zeta = 1/\sqrt{\pi} \text{ kg m}^2 \text{ s}^{-4}$, t_n defines the pulse duration, R is the input impedance of the receiver and \mathcal{E}_b the received energy per bit.

A. Large Number of Combined Pulses

The following calculations are based upon the receiver architecture (b). We note, that for a large number of combined pulses, the statistical properties of the timing errors completely determine the expected summed signal $r_{\text{sum}}(t)$. Therefore, it is not required to consider each timing error ε_j individually to calculate the summed signal and hence the BER performance. At the limit $N_f \rightarrow \infty$ and assuming that ε_j is mean ergodic, we have shown in [12] that the expected normalized summed signal without noise can be written as

$$\chi(t) \doteq \lim_{N_f \rightarrow \infty} \mathbb{E} \left[\frac{s_{\text{sum}}(t)}{N_f} \right] = p(t) * f(t) \quad (10)$$

where $\mathbb{E}[\cdot]$ denotes statistical expectation, $f(\varepsilon_j)$ is the probability density function (pdf) for the timing error ε_j , and $*$ denotes the convolution operator. Note that assuming ε_j to be mean ergodic is not a very restrictive assumption, as it can be shown that a sufficient condition for a discrete-time white-sense stationary (WSS) random process ε_j to be mean ergodic is $C_{\varepsilon_j}(0) < \infty$ and $\lim_{j \rightarrow \infty} C_{\varepsilon_j} = 0$ where C_{ε_j} is the covariance of ε_j [13]. Calculating (10) for the pulse shape defined in (9) and the jitter distribution (8), $\chi(t)$ is a 2nd derivative Gaussian pulse with increased duration

$$\chi(t) = A (t^2 - (\sigma^2 + t_n^2)) \exp \left(-\frac{1}{2} \frac{t^2}{\sigma^2 + t_n^2} \right) \quad (11)$$

and with an amplitude

$$A = \sqrt{\frac{4\zeta R \mathcal{E}_b}{3N_f}} \left(\frac{t_n}{\sigma^2 + t_n^2} \right)^{5/2}. \quad (12)$$

By selecting the locally generated template to be matched to the expected received pulse shape $h(t) = \chi(t) - \chi(t - \delta)$, the expected received energy per bit is

$$\mathcal{E}_\chi = N_f^2 \int_{-\infty}^{\infty} \chi^2(t) dt. \quad (13)$$

We define a loss L_{te} that relates the expected SNR at the detector in a system with jitter to the SNR without jitter. For the 2nd derivative Gaussian pulse shape and a Gaussian jitter, it can be shown to be [12]

$$L_{\text{te}} = \frac{\mathcal{E}_b}{\mathcal{E}_\chi} = \left(\frac{\sqrt{\sigma^2 + t_n^2}}{t_n} \right)^5. \quad (14)$$

In the absence of jitter ($\sigma = 0$), the loss L_{te} becomes independent of the pulse width and is 0 dB. For any real valued standard deviation of the jitter, the loss is larger than 1 (or positive in a dB scale). We note, that the loss due to the Gaussian distributed jitter depends on the pulse duration t_n . As expected, pulses with short duration are more sensitive to Gaussian jitter than pulses with a longer duration. Figure 2 represents the loss L_{te} as a function of the jitter standard deviation for four values of the pulse duration t_n . For example, the loss L_{te} of the SNR at the detector is 2.42 dB for $t_n = 0.2$ ns and $\sigma = 0.1$ ns (a 2nd derivative Gaussian pulse with duration $t_n = 0.2$ ns has a -10 dB bandwidth of about

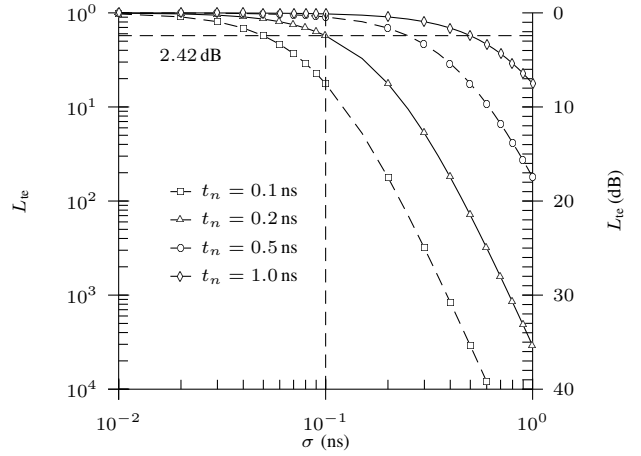


Fig. 2. Theoretical loss L_{te} for a 2nd derivative Gaussian pulse with duration t_n and a Gaussian distributed timing jitter with standard deviation σ .

1.65 GHz and an arithmetic center frequency of 1.24 GHz). As the locally generated template $h(t)$ is matched to the expected received signal, we expect that the BER will be given by the well known equation for orthogonal modulations

$$\text{BER} = Q \left(\sqrt{\frac{\mathcal{E}_\chi}{N_0}} \right) \quad (15)$$

where \mathcal{E}_χ is defined in (13). To prove (15), we consider that the expected correlation value becomes independent of the individual timing errors and is identical to the expected energy per bit \mathcal{E}_χ . Therefore, (7) can be expressed as

$$\text{BER} = P(\mathcal{E}_\chi, N_0) \int \cdots \int_{-\infty}^{\infty} \prod_{j=1}^{N_f} f(\varepsilon_j) d\varepsilon_j. \quad (16)$$

If further all the ε_j are statistically independent, the BER is

$$\text{BER} = P(\mathcal{E}_\chi, N_0) \prod_{j=1}^{N_f} \int_{-\infty}^{\infty} f(\varepsilon_j) d\varepsilon_j \quad (17)$$

and because of the normalization of the pdf

$$\text{BER} = P(\mathcal{E}_\chi, N_0). \quad (18)$$

Inserting (6) to (18), the proposition is shown to be correct.

As a consequence, the BER performance curve as a function of the SNR (represented in a logarithmic scale) at the antenna is shifted horizontally by the loss L_{te} . This is what can be observed in figure 3, where the theoretical performance using (15) and (13) is represented and compared with numerical results obtained by Monte-Carlo simulations for $N_f = 50$. The numerical results are in excellent agreement with the analytical equations. For example, the BER performance curve for $\sigma = 0.1$ ns is shifted by 2.42 dB, as expected. We note, that the BER is not bounded for high SNR, but tends towards 0.

B. Small Number of Combined Pulses

For a small number of combined pulses, the discussion is separated between the low SNR and the high SNR domain.

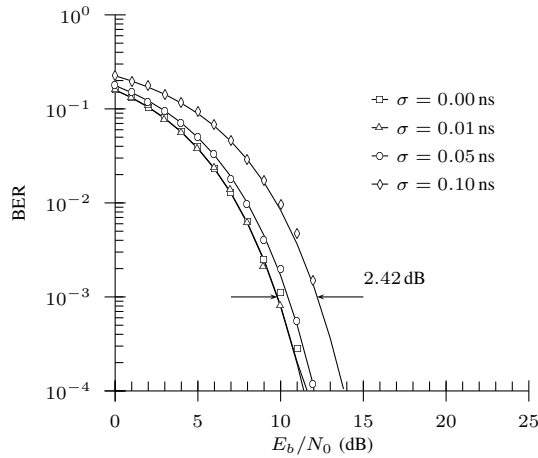


Fig. 3. BER as a function of the SNR in AWGN transmission channel for PPM in the presence of Gaussian jitter with standard deviation σ . The solid lines represent the theoretical results. The dots present the outcomes of Monte-Carlo simulations for $N_f = 50$.

The SNR is considered high, when the BER is dominated by the timing errors and the AWGN becomes negligible. On the other hand, the SNR is considered low, when the error probability due to the timing error becomes small compared to the error probability due to the interfering noise. However, even in the later case, the jitter is still considered to calculate the expected received energy per bit and to deduce the BER. For both domains, the discussion leads to a lower bound.

1) *High SNR*: If a data symbol is assumed to be 0 or 1, the detector estimates the most probable data symbol by

$$\hat{d}_0 = \frac{1}{2} [1 - \text{sign}\{C(\varepsilon_1, \dots, \varepsilon_{N_f})\}]. \quad (19)$$

Even for high SNR, the detector may take an erroneous decision due to a reversal of the correlation value under the influence of the timing errors. This result is in contrast to the case of a high number of combined pulse, where the BER tends towards 0 for high SNR. In the case of a noiseless transmission, (6) simplifies to the calculation of the sign of the correlation value and becomes

$$P(C(\varepsilon_1, \dots, \varepsilon_{N_f})) = \frac{1}{2} [1 - \text{sign}\{C(\varepsilon_1, \dots, \varepsilon_{N_f})\}]. \quad (20)$$

To calculate the correlation value, we assume the locally generated template to be $h(t) = \chi(t) - \chi(t - \delta)$. In the absence of timing errors, this template matches the received pulse shape and the receiver has optimum performance in AWGN. For a finite number of captured pulses with timing errors, the template is not matched to the received pulse shape. However, we have observed that the proposed template outperforms the template $h(t) = p(t) - p(t - \delta)$ in the presence of a Gaussian jitter. The application of the proposed template in a correlation receiver requires a priori knowledge about the clock jitter.

The results of the numerical estimation of the integrals obtained by combining (20) and (7) are represented in figure 4 for $1 \leq N_f \leq 5$. For example, for a single pulse ($N_f = 1$) and a Gaussian jitter with standard deviation 0.1 ns, the minimum BER is given by $2.44 \cdot 10^{-2}$ even in a noiseless transmission.

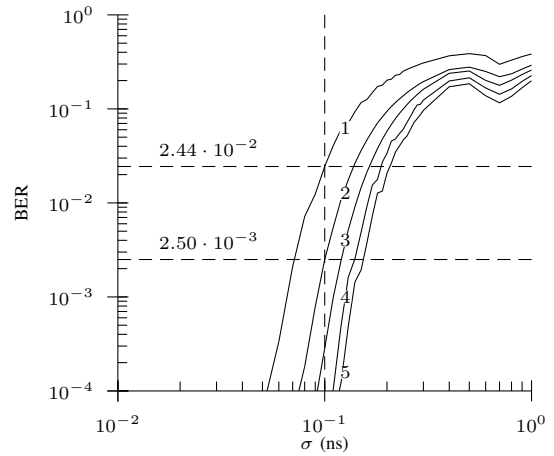


Fig. 4. BER as a function of the jitter standard deviation σ in a noiseless transmission for a 2nd derivative Gaussian pulse with $t_n = 200$ ps and $\delta = 2$ ns. The results are presented for N_f ranging from 1 to 5.

2) *Low SNR*: At low SNR, the influence of the noise becomes dominant. At the limit when the influence of the timing errors is neglected, the BER performance depends on the received energy \mathcal{E}_b . In this case, a lower bound BER_{B0} is given by

$$\text{BER}_{B0} = Q\left(\sqrt{\frac{\mathcal{E}_b}{\mathcal{N}_0}}\right). \quad (21)$$

However, in the presence of non negligible timing errors, the BER performance will not approach the bound (21). Instead, it is observed (see figures 5, 6, and 7) that

$$\text{BER}_{B1} = Q\left(\sqrt{\frac{E\{C(\varepsilon_1, \dots, \varepsilon_{N_f})\}}{\mathcal{N}_0}}\right) \quad (22)$$

provides a more accurate lower bound for the BER performance for low SNR. For the locally generated template $h(t) = \chi(t) - \chi(t - \delta)$ and assuming that the timing errors are mean ergodic, the expected correlation value becomes identical to the expected energy per bit $E\{C(\varepsilon_1, \dots, \varepsilon_{N_f})\} = \mathcal{E}_\chi$ estimated in (13). Equation (22) then becomes identical to (15). However, while (15) provides a closed form solution for the BER performance for an infinite number of combined pulses, (22) provides a lower bound that is only valid if the error probability due to the timing errors is small compared to the error probability due to the AWGN. By comparing the bound (22) with the BER performance (7) written using the expectation operator,

$$\text{BER} = E\left\{Q\left(\sqrt{\frac{C(\varepsilon_1, \dots, \varepsilon_{N_f})}{\mathcal{N}_0}}\right)\right\}, \quad (23)$$

we note that the bound (22) can be motivated for the domain where $y = Q(\sqrt{x})$ is approximately affine, i.e., for sufficient low SNR.

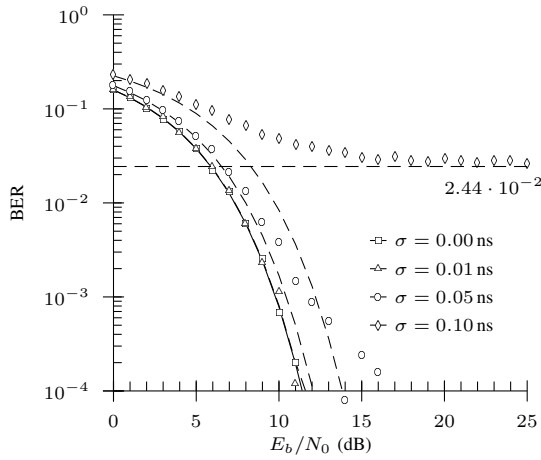


Fig. 5. BER as a function of the SNR in an AWGN transmission channel for PPM in the presence of Gaussian jitter with standard deviation σ . Numerical results obtained for $N_f = 1$. The dashed lines represent the bounds for high and low SNR.

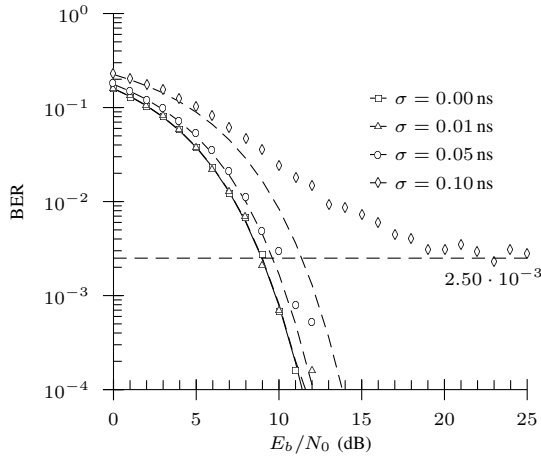


Fig. 6. BER as a function of the SNR in an AWGN transmission channel for PPM in the presence of Gaussian jitter with standard deviation σ . Numerical results obtained for $N_f = 2$. The dashed lines represent the bounds for high and low SNR.

3) *Comparison to Numerical Simulation:* The outcomes of Monte-Carlo simulations are compared to the bounds for high SNR and for low SNR. Figures 5, 6, and 7 present the results for $N_f = 1$, $N_f = 2$, and $N_f = 10$ respectively. The results from the numerical simulations approach asymptotically the lower bounds.

IV. CONCLUSION

In this paper, the BER performance for impulse radio in the presence of Gaussian jitter is provided for a 2nd derivative Gaussian pulse. The discussion starts with an analytical calculation of the expected SNR for a large number of combined pulses. The result is applied to derive a closed form solution for the expected BER. The analytical solution is compared to the outcomes of Monte-Carlo simulations. For a finite number of pulses, lower bounds for the BER performance are provided for low SNR and high SNR domains. Using

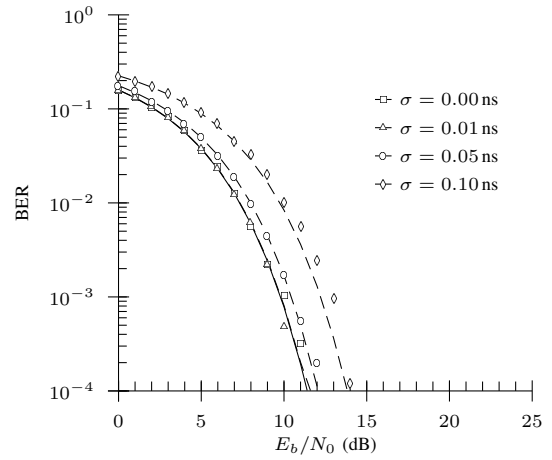


Fig. 7. BER as a function of the SNR in an AWGN transmission channel for PPM in the presence of Gaussian jitter with standard deviation σ . Numerical results obtained for $N_f = 10$. The dashed lines represent the bounds for high and low SNR.

numerical simulations, it is shown that the BER asymptotically approaches the estimated bounds. The provided results can be applied to estimate an upper bound for the jitter variance when a BER requirement for an impulse radio communication system is provided.

ACKNOWLEDGMENT

The authors are grateful to the Swiss National Science Foundation (<http://www.snsf.ch>) who supports this work under grant 200020-113472.

REFERENCES

- [1] M. Z. Win and R. A. Scholtz, "Impulse radio: How it works?" *IEEE Communications Letters*, vol. 2, no. 2, pp. 36–38, Feb. 1998.
- [2] M. Z. Win, "Spectral density of random time-hopping spread-spectrum uwb signals with uniform timing jitter," in *Military Communications Conference*, vol. 2, Atlantic City, NJ, USA, Nov. 1999, pp. 1196–1200.
- [3] —, "A unified spectral analysis of generalized time-hopping spread-spectrum signals in the presence of timing jitter," *IEEE Journal on Selected Areas in Communications*, vol. 20, no. 9, pp. 1664–1676, Dec. 2002.
- [4] İ. Güvenç and H. Arslan, "Performance evaluation of uwb systems in the presence of timing jitter," in *IEEE Conference on Ultra Wideband Systems and Technologies*, Reston, VA, USA, Nov. 2003, pp. 136–141.
- [5] S.-C. Lin and T.-D. Chiueh, "Performance analysis of impulse radio under timing jitter using m-ary bipolar pulse waveform and position modulation," in *IEEE Conference on Ultra Wideband Systems and Technologies*, Reston, VA, USA, Nov. 2003, pp. 121–125.
- [6] M. Pelissier, B. Denis, and D. Morche, "A methodology to investigate uwb digital receiver sensitivity to clock jitter," in *IEEE Conference on Ultra Wideband Systems and Technologies*, Reston, VA, USA, Nov. 2003, pp. 126–130.
- [7] İ. Güvenç and H. Arslan, "On the modulation options for uwb systems," in *Military Communications Conference*, vol. 2, Boston, MA, USA, Oct. 2003, pp. 892–897.
- [8] L. B. Michael, M. Ghavami, and R. Kohno, "Effect of timing jitter on hermite function based orthogonal pulses for ultra wideband communication," in *Wireless Personal Multimedia Communications, 4th International Symposium on*, Aalborg, Denmark, 2001.
- [9] J. Forgáč and P. Farkaš, "Analysis of different uwb systems with timing jitter and isi in awgn channel," in *Joint IST Workshop on Mobile Future and Symposium on Trends in Communications*, Bratislava, Slovakia, Oct. 2003, pp. 51–54.

- [10] W. M. Lovelace and J. K. Townsend, "The effects on timing jitter and tracking on the performance of impulse radio," *IEEE Journal on Selected Areas in Communications*, vol. 20, no. 9, Dec. 2002.
- [11] J. G. Proakis, *Digital Communications*, 4th ed. McGraw-Hill Higher Education, 2001.
- [12] R. Merz, C. Botteron, P.-A. Farine, and J. Farserotu, "Asymptotical analysis of timing imperfections in uwb receivers," in *IEEE Conference on Circuits and Systems for Communications*, Moscow, Russia, July 2004.
- [13] Y. Viniotis, *Probability and Random Processes for Electrical Engineers*. McGraw-Hill, 1997.